First publ. in: The Journal of Physical Chemistry C ; 115 (2011), 30. - pp. 15081-15088

THE JOURNAL OF PHYSICAL CHEMISTRY C

ARTICLE

pubs.acs.org/JPCC

Characterization of Interfacial Modifiers for Hybrid Solar Cells

Jonas Weickert,[†] Florian Auras,[‡] Thomas Bein,[‡] and Lukas Schmidt-Mende*[,†]

[†]Department of Physics and Center for NanoScience (CeNS), Ludwig-Maximilians-University Munich, Amalienstr. 54, D-80809 Munich, Germany

[‡]Department of Chemistry and Center for NanoScience (CeNS), Ludwig-Maximilians-University Munich, Butenandtstr. 5-13, 81377 Munich, Germany

Supporting Information

ABSTRACT: This study systematically investigates the influence of different TiO_2 surface modifiers on the device properties of TiO_2—poly(3-hexylthiophene) (P3HT) hybrid solar cells to infer design rules for interfaces in hybrid solar cells. Bare TiO_2 is compared to TiO_2 modified with a Ru(II) dye (Z907), phenyl-C_{61}-butyric acid (PCBA), the carboxylated polymer poly[3-(5-carboxypentyl)thiophene-2,5-diyl] (P3HT-COOH), and Sb_2S_3, respectively. Self-assembled monolayers are investigated for the former three modifiers, whereas a thin coating of only a few nanometers is used in the case of Sb_2S_3. Photoluminescence quenching analysis is performed for the different TiO_2—P3HT interfaces to gain insight into the mechanism of charge separation. For further analysis, the different modifiers are tested in solar cells. We focus on bilayered devices with a well-defined near-planar TiO_2—P3HT interface for easier data analysis. Absorption of light by the modifiers can thus be neglected. In addition, detailed current density—voltage curve analysis, photovoltage, and photocurrent decay measurements reveal mechanisms of charge carrier recombination and extraction. Our study underlines the importance of recombination control and matching energy levels as well as proper alignment of P3HT at the interface.

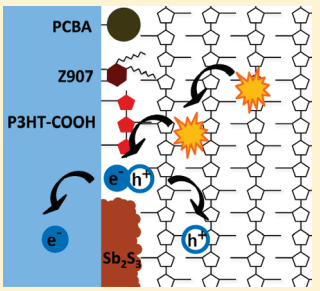

1. INTRODUCTION

Excitonic solar cells are a promising technology to compete with conventional Si-based photovoltaics and to meet the global demand for clean energy in the future. To date, dye-sensitized solar cells (DSSCs) based on liquid electrolytes as introduced by Grätzel in 1991 exhibit the highest power conversion efficiencies—beyond 11% under solar illumination.[1,2] However, liquid compounds include the risk of leaks in the device and corrosion, and flexible solar cells cannot be realized. On the other hand, solid state DSSCs based on transparent hole conductors like 2,2′,7,7′-tetrakis-(*N*,*N*-di-*p*-methoxyphenylamine)9,9′-spirobifluorene (Spiro-OMeTAD) cannot compete with their liquid electrolyte counterparts yet and show power conversion efficiencies (PCEs) that are still at the order of 5%.[3] High power conversion efficiencies beyond 8% have also been realized with the so-called bulk heterojunction (BHJ) concept where thin films of all-organic donor and acceptor materials, most commonly p-type polymers and n-type fullerenes, are fabricated in a mixed phase of the compounds, usually by spincoating from a blended solution.[4] Mainly, highly absorbing p-type polymers are mixed with electron-accepting fullerenes.[5,6] BHJs are supposed to form network-like morphologies with high interfacial area and good percolation pathways for electrons and holes.[7−9] However, control over this morphology is strongly limited, and even though domain sizes comparable to exciton diffusion lengths have been realized, charge carrier recombination due to incomplete pathways for one or both types of charge carriers becomes a severe problem if the active layer is significantly thicker than 100 nm. Internal quantum efficiencies (IQEs) approaching 100% have been shown for thin active layers, but high external quantum efficiencies (EQEs) also demand for strong absorption, i.e., thicker layers.[10] Due to nonideal morphologies, BHJ solar cells do not meet their theoretical predictions yet.[11]

A promising approach combining the advantages of DSSCs and the BHJ concept are so-called hybrid solar cells (HSCs).[12] A high surface area metal oxide nanostructure (commonly TiO_2 or ZnO), which replaces the organic electron acceptor, is infiltrated with absorbing polymers like poly(3-hexylthiophene) (P3HT) or polyphenylene vinylenes (PPVs), which serve as donor materials.[13−15] Thus, the morphology of the donor—acceptor interface can be controlled via the geometry of the metal oxide, and good percolation pathways can be established. Especially the use of ordered structures like nanowires or nanotubes is promising since control over structural geometry is possible and electron transport can be directed along one dimension over several micrometers which reduces charge carrier recombination.[16−18] HSCs therefore may overcome morphological limitations of the BHJ concept and allow thicker active layers. This should lead to full harvesting of incident photons. However, even though the concept is appealing, HSCs cannot yet compete with BHJ solar cells or DSSCs. During the past few years, several studies have dealt with this topic. It was suggested that the most likely reason

Received: April 18, 2011
Revised: June 22, 2011
Published: June 27, 2011

 © 2011 American Chemical Society

Konstanzer Online-Publikations-System (KOPS)
URN: http://nbn-resolving.de/urn:nbn:de:bsz:352-179667

for the relatively low efficiency of HSCs is that fullerenes, which are predicted to allow power conversion efficiencies of 10% in combination with suitable polymers, still work better as electron acceptors than TiO_2 or ZnO.[19] Therefore, sophisticated surface treatments of the metal oxides are necessary to enhance the probability of charge separation at the organic−inorganic interface and thus the efficiency of the solar cell. Goh et al. systematically investigated the influence of surface modifiers in TiO_2−P3HT bilayer solar cells and compared them to three Ru(II) dyes known from applications in DSSCs.[20] They were able to influence the resulting open circuit voltage (V_{OC}) by changing the effective work function of the TiO_2 via different dipoles introduced at the interface. Besides, they pointed out that alkyl chains attached to the dye can act as spacers between the TiO_2 and the polymer which significantly slow down charge carrier recombination. In 2009, Mor et al. were able to show a new record efficiency for TiO_2−dye−P3HT devices by introducing a monolayer of a near-IR absorbing dye onto nanotubular TiO_2.[21] A dramatic increase in performance (power conversion efficiency) from 0.3% to 3.8% was established when modifying the TiO_2 with the dye, which could not only be attributed to the broadened absorption spectra of the dye-sensitized HSCs due to additional near-IR absorption. Instead, they identified matching energy levels and a beneficial molecular structure of the dye as the main reason for the impressive efficiencies. Only recently, performances beyond 5% have been realized by Chang et al. using thin layers of Sb_2S_3 as surface modification in HSCs based on mesoporous TiO_2 and P3HT.[22] Sb_2S_3 seems to match nicely with the energy levels of TiO_2 and P3HT and allows high fill factors (FF) and short circuit currents (I_{SC}). However, photocurrent is generated mainly upon excitation of the strongly absorbing Sb_2S_3, whereas charge separation between Sb_2S_3 and P3HT seems to be neglectable.

There are still many open questions concerning the ideal TiO_2−organic interface. The optimal modifier is still unknown, even though a number of desired properties can be listed. The probability of charge separation has to be maximized to convert a high number of photons to charges by simultaneously maintaining low charge carrier recombination. The highest occupied molecular orbital (HOMO) and lowest unoccupied molecular orbital (LUMO) of the modifier should match with HOMOs and LUMOs of the conducting polymer and with the conduction and valence band of the TiO_2. Offset energies should be in the order of exciton binding energies to allow charge separation but still small enough to yield high V_{OC}. Ideally, the modifier itself is absorbing, thus allowing for better light harvesting.

Here, we exemplarily investigate four different surface modifiers for TiO_2−P3HT hybrid photovoltaic cells. We focus on mechanisms of charge separation and recombination and attribute the results directly to the properties of the different modifiers. For easier data analysis, we focus on bilayered solar cells with a flat, distinct TiO_2−polymer interface. Thus, also the absorption of the modifiers is small. Besides, there are no issues of incomplete polymer infiltration into nanostructures. Due to the small exciton diffusion lengths in P3HT, which are supposed to be in the order of 5−10 nm, only low efficiencies can be realized in our bilayered geometry. However, findings of this study can be directly applied to nanostructured HSCs, where the geometry of TiO_2 better matches with the exciton diffusion length of P3HT. Besides untreated TiO_2, we investigate self-assembled monolayers of the Ru(II) dye *cis*-RuLL′(SCN)2 (L = 4,4′-dicarboxylic-acid-2,2′-bipyridine, L′ = 4,4′-dinonyl-2,2′-bipyridine) (Z907), which has been shown to allow high efficiencies and reduced recombination in solid state DSSCs.[23] Additionally, a carboxylated P3HT, poly[3-(5-carboxypentyl)-thiophene-2,5-diyl] (P3HT-COOH), is used as an interface modifier which is also supposed to form monolayers due to binding of COOH to TiO_2. The material carries a carboxylic group at the end of each alkyl chain of P3HT and was shown to allow efficient charge generation and high photocurrent in HSCs based on mesoporous TiO_2 and P3HT.[24] The third interfacial layer investigated in this study is phenyl-C_{61}-butyric acid (PCBA), a fullerene derivative similar to 1-(3-methoxycarbonyl)propyl-1-phenyl6,6C_{61} (PCBM) which is also modified with a carboxylic group and can therefore bind to TiO_2. Vaynzof et al. were using PCBA on ZnO which yielded improved short circuit current density (I_{SC}), open circuit voltage (V_{OC}), and fill factor (FF) resulting in an overall increased PCE.[25] We also investigate the properties of Sb_2S_3 coatings on TiO_2 since the material has shown promise in nanostructured next-generation solar cells.[14,22] Sb_2S_3 shows a strong and broad absorption in the visible allowing for efficient photon harvesting in photovoltaics.[26] Sb_2S_3−P3HT solar cells therefore might combine the benefits of HSCs with the extremely thin absorber (ETA) approach, where nanostructures are coated with nanometer thin layers of strong absorbers and infiltrated with transparent (high bandgap) hole conductors like CuSCN.[27] In this study, however, we are mainly interested in the properties of Sb_2S_3 as an interface modifier which enables charge separation between P3HT and TiO_2. We therefore focus on very thin layers with negligible absorption resulting in P3HT being the main absorber in our system.

2. EXPERIMENTAL SECTION

Device Fabrication. Indium tin oxide (ITO) coated glass substrates (Kintech, 10 Ω/□) and glass slides were successively cleaned in ultrasonic baths of deionized water with commercial dishwashing fluid, acetone, and isopropanol for 15 min each, rinsed with ethanol, and dried in a nitrogen stream. Samples were further cleaned in an oxygen plasma for 7 min. Thin layers of TiO_2 were deposited onto the samples via spray-pyrolysis from a 1:10 solution of di-isopropoxytitanium bis(acetylacetonate) in ethanol (EtOH) at 450 °C. After spray pyrolysis, samples were kept at 450 °C for 15 min and cooled in air at a cooling rate of 3 °C/min. TiO_2 layers were approximately 100 and 10 nm thick for solar cell samples and glass slides, respectively. TiO_2 was immersed in a 20 mM aqueous solution of $TiCl_4$ for 18 h at room temperature, carefully rinsed with water, and again heated at 450 °C for 15 min. For monolayer attachment, samples were placed vertically in solutions of the materials for 48 h (Z907: 40 mM in ethanol (EtOH); P3HT-COOH: 1 mg/mL in dimethylformamide; PCBA: 0.2 mg/mL in chlorobenzene (CB)). Sb_2S_3 was deposited for 10 min from a chemical bath as described elsewhere.[16] Sb_2S_3 was heated at 325 °C for 30 min in nitrogen atmosphere and slowly cooled to room temperature before being exposed to ambient air. Prior to spincoating with P3HT, all dye-sensitized samples were rinsed with the respective solvents, and the samples with nonsensitized TiO_2 were heated at 150 °C for 5 min to remove adsorbed water. For solar cells, P3HT (Merck Chemicals) was spincoated from a 30 mg/mL solution in CB at 1200 rpm. On glass slides, P3HT was spincoated from a 4 mg/mL solution in CB at 3000 rpm. For solar cells, a thin layer of PEDOT:PSS (Clevios) was spray-deposited from a 1:10 solution in isopropanol as described elsewhere.[38] PEDOT:PSS was dried at 140 °C for 1 min in ambient air. Ag top contacts were DC

sputter-deposited at a rate of approximately 0.08 nm/s from Ar plasma with 1×10^{-2} mbar. The complete samples (solar cells and glass slides) were annealed again at 140 °C for 1 min in ambient atmosphere to improve the contact between the individual layers.

Device Characterization. Absorption spectra were acquired in transmission mode in an Agilent Technologies 8453 UV−vis spectrometer. PL measurements were performed with a Horiba Jobin Yvon Fluorolog spectrometer with a 500 W halogen lamp. A Keithley 2400 SourceMeter was used for current density−voltage (*IV*) and EQE characterization and controlled with a self-written LabView program. Cells were illuminated through a shadow mask with a resulting active area of 0.125 cm^2. A Fraunhofer Institute certified Si reference solar cell with a KG5 filter was used for calibration. For EQE measurements a LOT-Oriel Omni 150 monochromator in combination with a 150 W Xe lamp was used. *IV* characterization under illumination was performed using a LOT-Oriel LS0106 solar simulator. By linear fits to *IV* curves under solar illumination, series and shunt resistances are determined as slopes of these fits. For series and shunt resistances, the curve is fitted at moderate forward and reverse bias, respectively. For photovoltage decay (PVD) and photocurrent decay (PCD) measurements, a pulsed laser (10 Hz, 532 nm) was focused onto the tested sample. The sample was background-illuminated with a LOT-Oriel LS0106 solar simulator with a light intensity of approximately 60 mW/cm^2. Signals were recorded with a Tekscope DPO 7254 digital oscilloscope. Termination resistances 1 MΩ and 50 Ω were used for PVD and PCD measurements, respectively.

3. RESULTS AND DISCUSSION

3.1. Photoluminescence. To gain insight into the mechanism of charge separation at the TiO_2−P3HT interface upon excitation of the polymer, photoluminescence (PL) quenching measurements were conducted. PL quenching experiments were suggested as a valuable tool to estimate exciton diffusion lengths and the efficiency of charge separation or population of charge transfer states.[28,29] PL samples were realized on thin TiO_2 (∼10 nm) to avoid artifacts and interference effects.[30] As a reference, P3HT was spincoated onto a glass slide without TiO_2. Since P3HT layers were only 5−10 nm in thickness, most excitons in the P3HT are generated within the exciton diffusion length away from the TiO_2.

PL emission spectra for the different TiO_2 modifications resulting from excitation of the P3HT at 500 nm are shown in Figure 1. Spectra are normalized to the optical density of the respective sample at 500 nm. The highest PL is exhibited by the control sample with P3HT on glass. If applied on TiO_2 with or without surface modifications, the PL of P3HT is significantly quenched, which is attributed to excitons either being converted to charge transfer states at the interface or being completely separated to free charge carriers. Since recombination of both charge transfer states and free charge carriers is supposed to be either nonradiative or exhibiting different emission spectra than recombination of excitons, this is a hint that excitons are energetically modified at the interface and might be separated into free charges.

The most efficient PL quenching of the P3HT layer results from PCBA modification of TiO_2, whereas higher PL intensities are detected for Z907 and P3HT-COOH. This suggests that population of charge transfer states and charge separation is most

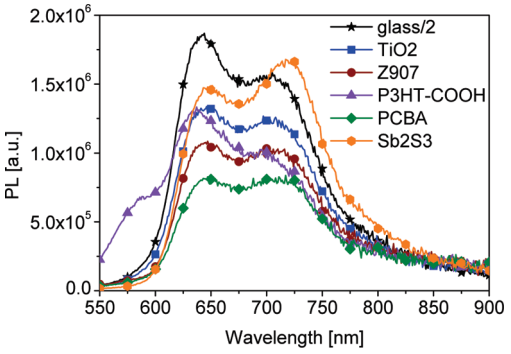

Figure 1. Photoluminescence emission spectra of P3HT on TiO_2 with different modifications. Excitation wavelength was 500 nm. The presented spectra are proportional to counts of emitted photons at the specified wavelength. For P3HT on a glass substrate without TiO_2 or any modifier, the spectrum is devided by a factor of 2 (indicated by the label "glass/2" for easier reading of the other spectra); i.e., twice as many counts were detected than represented in the graph.

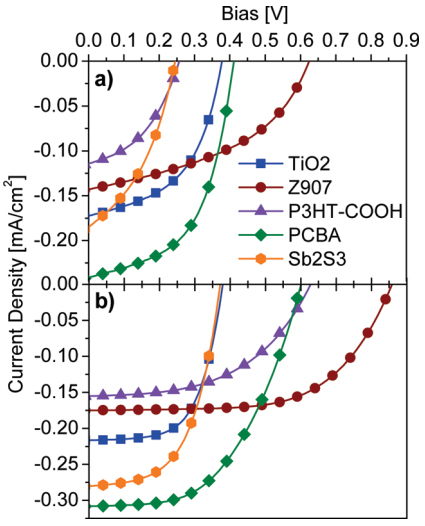

Figure 2. (a) Current density−voltage characteristics of bilayered devices with different TiO_2 modifications tested under simulated AM 1.5G illumination at 100 mW/cm^2. (b) Current density−voltage curves acquired in the dark shifted by the reverse saturation photocurrent under 1 sun illumination (estimated from the current density under solar illumination at −0.5 V).

efficient for PCBA. Nevertheless, Z907 and P3HT-COOH exhibit more efficient PL quenching than bare TiO_2, suggesting that charge separation at a neat TiO_2−P3HT interface is insufficient. In the case of P3HT-COOH, covalent binding of the material to the TiO_2 seems to enhance charge transfer between the donor and acceptor. However, P3HT-COOH shows a slightly different shape of its emission spectrum. We attribute this to the PL of P3HT-COOH itself. During the sensitization process, different P3HT-COOH strands compete for the available binding sites on TiO_2. Therefore, single strands might attach only with a certain fraction of their carboxylic linkers, whereas the rest of the strand points away from the substrate and coils with other strands. Effectively, there is more than only a monolayer of thiophenes on top of TiO_2 which then contribute a significant PL to the overall spectrum. A higher PL

Table 1. V_{OC}, I_{SC}, FF, R_{shunt}, R_{series}, and PCE for Different TiO_2 Modifications

cell type	V_{OC} [V]	I_{SC} [mA/cm^2]	FF [%]	R_{shunt} [kΩ·cm^2]	R_{series} [Ω·cm^2]	PCE [‰]
TiO_2	0.36 ± 0.02	0.16 ± 0.03	49.0 ± 1.3	10.2 ± 2.5	36.3 ± 3.6	0.28 ± 0.06
Z907	0.57 ± 0.03	0.13 ± 0.01	44.4 ± 3.5	12.2 ± 1.2	69.4 ± 9.9	0.32 ± 0.05
P3HT-COOH	0.25 ± 0.04	0.10 ± 0.02	42.5 ± 1.3	9.6 ± 1.5	58.9 ± 7.5	0.11 ± 0.04
PCBA	0.40 ± 0.01	0.22 ± 0.02	53.2 ± 2.6	10.4 ± 0.1	38.9 ± 2.8	0.46 ± 0.06
Sb_2S_3	0.23 ± 0.03	0.17 ± 0.02	40.7 ± 1.3	4.4 ± 0.8	25.8 ± 2.3	0.16 ± 0.03

contribution at smaller wavelengths is also consistent with the idea of coiled (and therefore noncrystalline) P3HT-COOH strands. A coiled structure might inhibit interchain interactions and trap excitons, which are consequently less efficiently quenched. Disordered (regiorandom) polythiophenes have been reported to absorb and emit more in the blue than ordered (regioregular) polythiophenes.[31] We therefore attribute the additional PL at lower wavelengths to disordered P3HT-COOH. Besides, coiled P3HT-COOH residues might induce a less-ordered structuring of the P3HT which is in direct contact with the interface and accordingly also emits at higher energies. Nevertheless, PL quenching around 725 nm is more efficient for P3HT-COOH than for Z907, suggesting that P3HT-COOH promises high charge separation yield if coiling of the polymer strands could be avoided.

The highest PL in our study is exhibited in the case of Sb_2S_3. Although being only a few nanometers thick, the Sb_2S_3 layer shows a slight PL emission. Therefore, we corrected the signal by the emission of Sb_2S_3 without P3HT on top. Nevertheless, the resulting spectrum is normalized to the overall absorption of the sample, and the PL of P3HT is therefore probably still slightly underestimated. This result suggests that there are significantly less charge transfer states at the Sb_2S_3−P3HT interface than for other modifiers investigated in this study. This might be due to nonmatching energy levels of the involved materials. However, since all our samples are processed in air, we mainly attribute the lower PL quenching to a thin Sb_2O_3 layer between Sb_2S_3 and P3HT which instantly forms if Sb_2S_3 is exposed to air.

From PL measurements, the most efficient exciton separation is expected for PCBA, whereas Sb_2S_3 as the interfacial layer seems to be detrimental even when compared to nonmodified TiO_2. This is mainly attributed to the presence of Sb_2O_3 on top of Sb_2S_3. In turn, matching energy levels and intimate contact between P3HT and the surface modifier seem to promote charge separation. The alkyl side chains of Z907 are probably spacing apart donor and acceptor leading to less efficient PL quenching than PCBA. P3HT-COOH seems to allow efficient charge separation, probably because exciton transfer between P3HT and P3HT-COOH is possible and covalent binding of P3HT-COOH to TiO_2 leads to fast electron injection. However, misalignment of P3HT and insufficient binding of P3HT-COOH to TiO_2 lead to nonoptimized PL quenching.

Note that P3HT shows an overall weak PL emission even on glass when no quenching at a charge separating interface is possible. Most excitons generated in P3HT relax nonradiatively, which is not the case for other p-type polymers like PPVs, where even the intensity of the emission of charge transfer states is still detectable.[32] In the case of P3HT, however, population of charge transfer states or complete separation of these excitons cannot be monitored by PL measurements. Nevertheless, the emission spectrum of P3HT resembles the absorption spectrum and is mainly shifted to the red, suggesting that a small fraction of excitons of all possible energies contribute to the PL.

3.2. Current Density−Voltage Characterization. To investigate the properties of the different modifiers in solar cells, we built bilayered devices with the structure ITO−TiO_2−Modifier−P3HT−PEDOT:PSS−Ag. Typical current density−voltage (*IV*) curves under illumination with simulated AM 1.5G light at 100 mW/cm^2 are shown in Figure 2 a), and characteristics are summarized in Table 1. Mean values and standard deviations are given for six individual solar cells of each type. The highest V_{OC} is exhibited by Z907 samples, which in turn show slightly lower photocurrents than untreated TiO_2. PCBA allows the highest I_{SC} and FF which is in good concordance with the pronounced PL quenching. Only a low V_{OC} is achieved with P3HT-COOH and Sb_2S_3. Note that higher V_{OC} and photocurrents up to several milliamperes are achieved for thicker layers of Sb_2S_3 (see Supporting Information). However, in this case charge carriers are supposed to be mainly generated upon excitation of the Sb_2S_3. External quantum efficiency (EQE) spectra normalized to resulting photocurrents resemble each other and follow the absorption spectrum of P3HT for the five different TiO_2 surfaces used in this study. In contrast, if thicker Sb_2S_3 is used, the shape of the EQE spectrum changes significantly and no longer reflects prominent P3HT features (see Supporting Information). As supported by PL measurements (see above), this suggests only poor charge injection from P3HT into Sb_2S_3. Since we focus on charge separation between P3HT and TiO_2, we are using only thin layers of Sb_2S_3 with very low absorption. Note, however, that due to the broad absorption spectrum of Sb_2S_3 it is not possible to exclude that there is current contribution from Sb_2S_3 to the EQE. The higher photocurrent for Sb_2S_3 than for untreated TiO_2 might therefore also be caused partly by the Sb_2S_3 itself.

All cells show relatively low performances, even when compared to bilayered cells with similar compounds as reported by Goh et al.[20] However, instead of processing and measuring inside a nitrogen glovebox, which is highly expensive for potential upscaling, our fabrication as well as all measurements are performed in ambient atmosphere. Besides, our P3HT layers are approximately 150 nm thick. This simplifies data analysis since light reflected at the top contacts can be neglected. Note, however, that significant improvements of device performance are possible if more light is reflected and optical spacers are used to achieve a maximum field intensity at the charge-separating interface, especially in the case of a bilayered solar cell.[33] Additionally, Goh et al. used a different synthesis route for TiO_2.

Although providing large shunt resistances (R_{shunt}) in the order of 10 kΩ·cm^2, all devices suffer from leakage currents under solar illumination which are relatively high with respect to the photocurrents. This significantly affects the FF which does not exceed 53% for any of the modifications. Besides, relatively large series resistances (R_{series}) are found. This is partly attributed to a decrease in ITO conductivity during spray pyrolysis of TiO_2 at

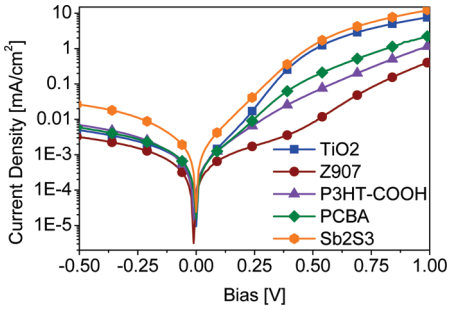

Figure 3. Current density−voltage characteristics of bilayered devices with different TiO_2 modifications tested in the dark.

450 °C. Additionally, for concerns of reproducibility and stability of devices, we chose a P3HT thickness of approximately 150 nm. This relatively thick layer might also contribute to R_{series}.

Figure 2(b) shows *IV* curves obtained from shifting curves measured in the dark by the reverse saturation photocurrent which was estimated from the current at −0.5 V. The resulting curves represent idealized *IV* response in the absence of photoshunts and at optimized charge separation without any recombination.[34] At −0.5 V, excitons are not only separated by the energy offset between donor and acceptor but also in the external electric field. Since the resulting virtual photocurrents are higher than I_{SC} values measured under solar illumination, we conclude that charge separation is nonideal for all TiO_2 modifications. However, the effect is less pronounced in the case of PCBA and Z907 than for Sb_2S_3 and P3HT-COOH, where the virtual I_{SC} increases by approximately 50%. Besides, the virtual V_{OC} differs significantly from the measured V_{OC} for some modifications. Especially for P3HT-COOH, a V_{OC} increase of 100% is found for the shifted dark curves compared to the 1 sun measurements. This suggests that P3HT-COOH enables pronounced charge carrier recombination upon illumination which reduces the V_{OC} and probably even the I_{SC}.

Complete dark curves are exemplarily shown in Figure 3 and suggest the presence of injection barriers introduced by some of the TiO_2 modifications. Good blocking at reverse bias and comparably low reverse currents are found for all modifications except Sb_2S_3. In contrast, there are significant differences in forward currents suggesting barriers for charge injection. All modifications except Sb_2S_3 allow systematically lower forward currents than bare TiO_2, which is also the case under 1 sun illumination (not shown). The presence of an additional material at the TiO_2−P3HT interface seems to slow down the recombination of holes from P3HT and electrons from TiO_2 at far forward bias, thus generating a space charge which limits charge injection and forward current.[35]

However, especially in the case of P3HT-COOH, this reduced recombination does not lead to a higher V_{OC} under 1 sun illumination. The shifted dark curve yields a V_{OC} which is significantly larger than for bare TiO_2 and does even exceed the V_{OC} of PCBA. The recombination limitations for P3HT-COOH apparent from low FF and V_{OC} under illumination seem to occur mainly at small bias. In concordance to PL data, we attribute this to randomly coiled P3HT-COOH strands close to the interface. These coils might provide traps for holes resulting from charge separation at the P3HT−TiO_2 interface. Holes cannot leave these traps toward the P3HT and thus serve as recombination centers which are easily accessible from the TiO_2. If this is the case, also the transfer of holes from P3HT to P3HT-COOH might be slowed down leading to low forward currents. Holes which are already located in P3HT-COOH coils recombine quickly with electrons from the TiO_2, whereas holes from P3HT are transferred slowly to P3HT-COOH and TiO_2. Besides, as discussed in the PL section, unordered P3HT-COOH might disturb crystallization of P3HT close to the interface resulting in lower hole mobilities.

In contrast, Z907, which exhibits the lowest forward currents, seems to slow down charge carrier recombination both in the dark and under illumination. This is in good accordance with earlier reports and is attributed to Z907's alkyl side chains which work as physical spacers between TiO_2 and P3HT. PCBA, which allows the highest photocurrents, also leads to the highest forward currents of all modifications, suggesting that both charge separation and injection work properly between P3HT and PCBA-modified TiO_2. This can be attributed to both intimate contact between P3HT and PCBA and matching energy levels of the materials. Besides, slightly lower forward currents for PCBA than for bare TiO_2 are in accordance with the slightly higher V_{OC} of PCBA.

The overall highest currents in both forward and reverse direction are exhibited by Sb_2S_3-modified TiO_2. Charge carrier recombination seems to be a serious issue for Sb_2S_3 devices, which show significantly reduced shunt resistances even in the dark. From experiments with thicker Sb_2S_3, we conclude that efficient charge separation between Sb_2S_3 and TiO_2 is possible, but recombination is also strong since we detect high photocurrents but low FF and R_{shunt}. Therefore, the characteristic of Sb_2S_3-modified TiO_2−P3HT devices is mainly determined by the Sb_2S_3−P3HT interface. Even though charge separation between Sb_2S_3 and P3HT seems to be insufficient compared to other modifiers, charge transfer across the P3HT−Sb_2S_3 interface seems to be quick, resulting in high dark forward currents. This is in good concordance with low R_{shunt}, V_{OC}, and FF found for Sb_2S_3-modified devices.

3.3. Transient Photocurrent and Photovoltage Decay Measurements. To further investigate the mechanisms of charge carrier extraction and recombination, transient photovoltage (PVD) and photocurrent decay (PCD) measurements are performed. Figure 4(a) shows PCD transients obtained for different TiO_2 modifications upon pulsed laser excitation at 532 nm and background illumination with a 60 mW/cm^2 solar simulator. The laser pulse generates additional photocharges, which can either recombine or exit the device via the external contacts and the oscilloscope's 50 Ω termination resistance. Charge carrier recombination as determined from PVD measurements (see below) is 50−100 times slower than the time scale for PCD. Therefore, PCD characteristics are mainly attributed to charge extraction. Laser intensity is adjusted via appropriate filters to yield similar peak values for the transient photocurrent which makes comparison of resulting signals easier for different TiO_2 modifications. PCD transients are appropriately fitted by a monoexponential function

$$I(t) = I_0 \cdot \exp(-k_{PCD} \cdot t) \quad (1)$$

where I_0 is the transient's amplitude and k_{PCD} the decay rate. Typical PCD lifetimes obtained as $\tau_{PCD} = 1/k_{PCD}$ are summarized in Table 2. Note that we find similar trends when exciting the tested devices all with a fixed laser intensity.

The shortest lifetimes are found for bare TiO_2 and PCBA, whereas charge carrier extraction is slightly slower for P3HT-COOH. This is

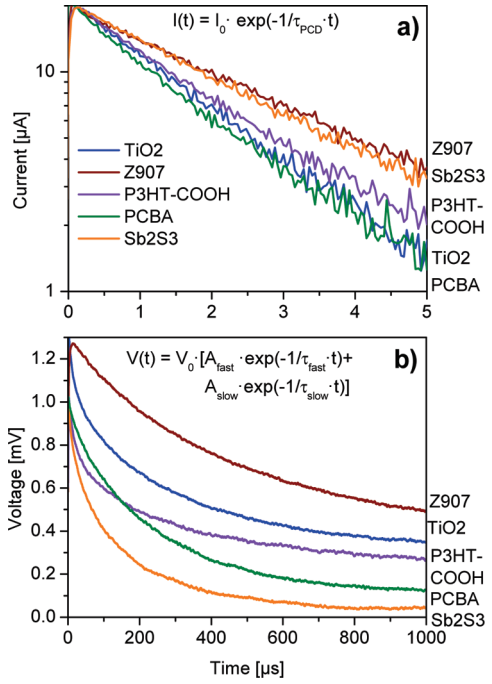

Figure 4. Transient signals of (a) photocurrent decay and (b) photovoltage decay measurements for devices with different TiO_2 modifications.

Table 2. Lifetimes and Proportional Amplitudes for PCD and PVD Data Resulting from Monoexponential and Biexponential Fitting, Respectively

cell type	τ_{PCD} [μs]	$\tau_{PVD,fast}$ [μs]	$A_{PVD,fast}$ [%]	$\tau_{PVD,slow}$ [μs]	$A_{PVD,slow}$ [%]
TiO_2	1.93	37.7	63.3	384.6	36.7
Z907	3.07	414.0	73.0	3906.1	27.0
P3HT-COOH	2.22	60.3	50.4	593.5	49.6
PCBA	1.91	118.1	86.5	1104.5	13.5
Sb_2S_3	3.12	79.6	74.5	296.1	25.5

in good accordance with the *IV* results discussed above. Charge separation is supposed to be comparably quick for bare TiO_2, PCBA, and P3HT-COOH. However, holes might get temporarily trapped in P3HT-COOH coils before being transferred to P3HT and transported to the Ag contact, which consequently causes a higher extraction lifetime. Compared to TiO_2, PCBA, and P3HT-COOH, slow charge extraction is found for Z907 and Sb_2S_3. Both modifications show extended transient photocurrents, which, however, still decay monoexponentially with time. Four mechanisms are conceivable, causing extended extraction times: (1) the presence of long-lived excited states leads to the generation of charge carriers late after the laser pulse, (2) charge transport is slow through the electron and/or the hole conductor, (3) injection barriers at one or both of the external contacts slow down transfer of charges from the photoactive material to the contacts, and (4) charges get quickly separated at the interface, but transfer of one or both types of charge carriers from the interface to the electron or hole conducting material is slow. For (1), an extended rise time of the photocurrent transient would be expected. Since this is not the case for Sb_2S_3 or Z907, we suppose that no long-lived excited states are present in our devices or play at least a very minor role. Furthermore, we exclude (2) and (3) since electron and hole conducting material as well as the external contacts are the same for all devices tested and cannot explain differences among the surface modifications. Accordingly, we suggest that charges, most likely holes, remain located close to the interface within the modifier, and transfer to P3HT is relatively slow.

On the basis of the HOMO and LUMO levels of P3HT and Z907, the mechanism of charge generation might contain an energy transfer from P3HT to Z907 and a subsequent charge separation between Z907 and TiO_2.[36,37] The hole then remains relatively long in the Z907 compared to other modifiers, which could be attributed Z907's alkyl side chains which physically separate the modifier from P3HT. As discussed above, for Sb_2S_3 charges might be separated at both interfaces, TiO_2—Sb_2S_3 and Sb_2S_3—P3HT. In either case, one type of charge carrier has to travel through the Sb_2S_3 (holes in the former, electrons in the latter case). Low charge carrier mobilities in the Sb_2S_3 might therefore cause the slower charge extraction compared to bare TiO_2 or PCBA.

To analyze recombination mechanisms for different modifiers, we also performed transient PVD measurements. In addition to an offset caused by background illumination with a solar simulator, a transient voltage signal is generated by a laser pulse, and the decay is monitored. Similar to PCD measurements, the laser intensity is adjusted to yield similar peak voltages. Again, the same trends as discussed here are found if devices are excited at a fixed laser intensity.

Since solar cells are held at quasi-open circuit conditions during the measurement by using the oscilloscope's 1 MΩ termination resistance, no charge carriers can exit the device, and recombination is the only mechanism which reduces the voltage to its equilibrium value after laser excitation. Note that since a PVD measurement detects only completely separated charge carriers, which have already reached the external contacts, not all recombination mechanisms present in organic or hybrid excitonic solar cells can account for the shape of the PVD transient.[34] Geminate recombination of excitons, i.e., recombination of the charge transfer state before its separation to free electron and hole, cannot be detected. Nevertheless, geminate recombination might be a major loss mechanism if charge separation occurs relatively late after population of charge transfer states or if free charges are moving away from the separating interface slowly.

All PVD transients found cannot be properly fitted using a single exponential function. We therefore choose a biexponential fit

$$V(t) = V_0 \cdot (A_{fast} \cdot \exp(-k_{fast} \cdot t) + A_{slow} \cdot \exp(-k_{slow} \cdot t)) \quad (2)$$

where V_0 is an amplitude; k_{fast} and k_{slow} are exponential rates for the fast and slow part of the decay, respectively; and A_{fast} and A_{slow} are proportionality factors determining the contribution of the fast and the slow exponential to the decay, respectively. Typical PVD lifetimes calculated as $\tau_{fast} = 1/k_{fast}$ and $\tau_{slow} = 1/k_{slow}$ as well as A_{fast} and A_{slow} are summarized in Table 2. At this point, the exact origin of the biexponential behavior is unknown. However, we suppose that the fast decay mainly determines the cell's properties at working conditions under solar illumination. There, charge generation and recombination

already are in equilibrium, and the fast mechanism should outcompete the slow mechanism.

The fastest recombination is found for bare TiO_2 in contact with the P3HT hole conductor, suggesting that the introduction of modifiers at the TiO_2−P3HT interface slows down charge transfer across the interface in either case. This partially explains the relatively low V_{OC} found for TiO_2, especially in the case of the shifted dark curve, where recombination due to photogenerated charge carriers is neglected. Fast recombination is also found for P3HT-COOH. This might be attributed to P3HT-COOH coils which trap holes and enhance surface state recombination.[34] Nevertheless, recombination is slower than for bare TiO_2, probably because P3HT-COOH coils provide a transport barrier for holes. Sb_2S_3 exhibits relatively fast recombination, which might account for the low V_{OC} found for this modifier. The precise nature of this quick recombination in combination with slow charge extraction for Sb_2S_3 is currently investigated in our group. However, PCD and PVD measurements are in good concordance with *IV* results and can partly explain low V_{OC} and FF.

Extended lifetimes are found for PCBA and especially for Z907, which both exhibit high V_{OC}. PCBA assembles between TiO_2 and P3HT with HOMO and LUMO aligning between the energy levels of TiO_2 and P3HT. This introduces an additional energetic step for electron and hole transfer, which guides separated charge carriers quickly away from the interface but slows down recombination as apparent from PCD and PVD data, respectively. For Z907, probably the same mechanism which slows down charge extraction is significantly reducing recombination. Z907 introduces a physical spacer between TiO_2 and P3HT, which can screen free electrons and holes and leads to slower recombination and high V_{OC}.

Note that due to its bulky character and low solubility full coverage of TiO_2 during sensitization with PCBA cannot be assured. This might result in P3HT being in direct contact with TiO_2 reducing recombination lifetimes and V_{OC}.

4. CONCLUSION

Four different surface modifiers were exemplarily tested in bilayered TiO_2−P3HT solar cells and compared to cells with untreated TiO_2. Even though Sb_2S_3 has shown great promise in nanostructured hybrid solar cells, this is most likely due to its own high absorption and energy levels which match nicely with TiO_2. If thicker Sb_2S_3 layers are used, which contribute significantly to the device absorption, highly efficient HSC can be realized as already shown by Chang et al.[1] In such devices, formation of a thin oxide layer on top of Sb_2S_3 seems to be beneficial since charge carrier recombination is reduced.[14,39] Even if crystallization of Sb_2S_3 is carried out in an inert atmosphere, samples are commonly cooled quickly in ambient air to yield controlled oxidation of the surface of the Sb_2S_3 layer. However, very thin layers of Sb_2S_3 with negligible absorption appear to be detrimental for device performance if this oxide layer is present since charge injection from the donor into TiO_2 is inhibited. The Sb_2O_3 very likely functions as a blocking layer at the interface, which on the one hand reduces charge carrier recombination but on the other hand does not allow charge injection from the hole transporting material. For a cell design as in the present study, where the surface modifier should promote charge injection, Sb_2S_3 seems not to be the material of choice. Even though interfacial coatings with highly absorbing materials hold promise for good light harvesting and high efficiencies, energy levels have to be adjusted carefully to avoid introduction of injection barriers. P3HT-COOH seems to be detrimental to device efficiency at least in bilayered devices. This is mainly attributed to a nonhomogenous coating of TiO_2 with the material, leading to P3HT-COOH coils, which serve as charge traps resulting in slower charge extraction and fast recombination. Besides, the low order of P3HT-COOH might induce low order of the adjacent P3HT in turn. In our study, the highest efficiencies are realized with Z907 and PCBA. The former allows high V_{OC} but lower photocurrents due to its alkyl side chains, which slow down charge carrier recombination but also lead to slower charge extraction. PCBA cannot compete with Z907's V_{OC} but significantly slows down charge carrier recombination compared to bare TiO_2. Moreover, the highest photocurrent can be realized with PCBA, which is attributed to the fullerene's outstanding properties as an electron acceptor.

From our results, we infer the following design rules for interfacial modifiers in metal oxide−polymer hybrid solar cells: (1) Energy levels of the interfacial modifier should be adjusted to allow either efficient charge injection or energy transfer from the hole conductor as shown for PCBA. The donor and interfacial modifier should be in intimate contact, and complete and homogeneous coverage of the metal oxide with the modifier should be established, which apparently was not the case for P3HT-COOH. (2) Physical spacers like alkyl side chains can help to efficiently reduce charge carrier recombination and enhance open circuit potential as found for Z907. However, charge or energy transfer should still be possible across the spacers to allow high photocurrents. (3) Surface modifiers have to be selected carefully to avoid introduction of charge traps at the interface as in the case of P3HT-COOH coils. Besides, high order and good crystallization of the polymer should not be disturbed by the modifier. (4) A combination of the hybrid concept and the principles of extremely thin absorber cells holds great promise. Dense, compact layers of highly absorbing interfacial layers like Sb_2S_3 can be realized. However, charge transfer and exciton separation should be possible between TiO_2 and the interfacial layer as well as between the interfacial layer and polymer, thus requiring matching energy levels.

Partial control over the hybrid solar cell's I_{SC} and V_{OC} is possible by choice of the appropriate modifier. Matching energy levels as in the case of P3HT and PCBA allow efficient exciton separation. In addition, our results can likely be transferred to different hole conductors like PPVs. Chemical modification of PCBA with alkyl side chains might offer a route toward further improving the efficiency of TiO_2−P3HT hybrid solar cells. Thus, high photocurrents could be combined with increased V_{OC}. Besides, molecules comprising PCBA with chemically bound dyes like Z907 might be interesting for future applications in hybrid photovoltaics. Such molecules might enable both energy transfer and subsequent charge separation as well as direct charge separation at the interface.

■ ASSOCIATED CONTENT

Supporting Information. Contents: External quantum efficiencies of solar cells with different TiO_2 modifications and current density−voltage curve of TiO_2−Sb_2S_3−P3HT solar cells with different Sb_2S_3 thicknesses. This material is available free of charge via the Internet at http://pubs.acs.org.

AUTHOR INFORMATION

Corresponding Author
*E-mail: l.schmidt-mende@physik.lmu.de.

ACKNOWLEDGMENT

We acknowledge support by the German Excellence Initiative of the Deutsche Forschungsgemeinschaft (DFG) via the "Nanosystems Initiative Munich (NIM)", the DFG in the program "SPP1355: Elementary processes of organic photovoltaics", and the Center for NanoScience (CeNS) Munich for support through the International Doctorate Program NanoBioTechnology (IDK-NBT). We thank Prof. Jochen Feldmann for access to laboratories and instruments.

REFERENCES

(1) Oregan, B.; Grätzel, M. *Nature* **1991**, *353*, 737.
(2) Hagfeldt, A.; Boschloo, G.; Sun, L.; Kloo, L.; Pettersson, H. *Chem. Rev.* **2010**, *110*, 6595.
(3) Snaith, H. J.; Schmidt-Mende, L. *Adv. Mater.* **2007**, *19*, 3187.
(4) Liang, L. Y. Y. *Acc. Chem. Res.* **2010**, *43* (9), 1227.
(5) Armstrong, N. R.; Wang, W. N.; Alloway, D. M.; Placencia, D.; Ratcliff, E.; Brumbach, M. *Macromol. Rapid Commun.* **2009**, *30*, 717.
(6) Blom, P. W. M.; Mihailetchi, V. D.; Koster, L. J. A.; Markov, D. E. *Adv. Mater.* **2007**, *19*, 1551.
(7) Hoppe, H.; Sariciftci, N. S. *J. Mater. Res.* **2004**, *19*, 1924.
(8) Hoppe, H.; Sariciftci, N. S. *Adv. Polym. Sci.* **2008**, *214*, 1.
(9) van Bavel, S. S.; Barenklau, M.; de With, G.; Hoppe, H.; Loos, J. *Adv. Funct. Mater.* **2010**, *20*, 1458.
(10) Park, S.; Roy, A.; Beaupré, S.; Cho, S.; Coates, N.; Moon, J.; Moses, D.; Leclerc, M.; Lee, K.; Heeger, A. *Nat. Photonics* **2009**, *3*, 297.
(11) Dennler, G.; Scharber, M. C.; Brabec, C. J. *Adv. Mater.* **2009**, *21*, 1323.
(12) Weickert, J.; Dunbar, R. B.; Wiedemann, W.; Hesse, H. C.; Schmidt-Mende, L. *Adv. Mater.* **2011**, *23*, 1810.
(13) Beek, W. J. E.; Wienk, M. M.; Janssen, R. A. J. *Adv. Mater.* **2004**, *16*, 1009.
(14) Itzhaik, Y.; Niitsoo, O.; Page, M.; Hodes, G. *J. Phys. Chem. C* **2009**, *113*, 4254.
(15) Zeng, T.; Lin, Y.; Lo, H.; Chen, C.; Chen, C.; Liou, S.; Huang, H.; Su, W. *Nanotechnology* **2006**, *17*, 5387.
(16) Feng, X. J.; Shankar, K.; Paulose, M.; Grimes, C. A. *Angew. Chem., Int. Ed.* **2009**, *48*, 8095.
(17) Mor, G.; Shankar, K.; Paulose, M.; Varghese, O.; Grimes, C. *Nano Lett.* **2006**, *6*, 215.
(18) Weickert, J.; Palumbiny, C.; Nedelcu, M.; Bein, T.; Schmidt-Mende, L. *Chem. Mater.* **2011**, *23*, 155.
(19) Scharber, M. C.; Wuhlbacher, D.; Koppe, M.; Denk, P.; Waldauf, C.; Heeger, A. J.; Brabec, C. L. *Adv. Mater.* **2006**, *18*, 789.
(20) Goh, C.; Scully, S. R.; McGehee, M. D. *J. Appl. Phys.* **2007**, 101.
(21) Mor, G.; Kim, S.; Paulose, M.; Varghese, O.; Shankar, K.; Basham, J.; Grimes, C. *Nano Lett.* **2009**, *9*, 4250.
(22) Chang, J.; Rhee, J.; Im, S.; Lee, Y.; Kim, H.; Seok, S.; Nazeeruddin, M.; Gratzel, M. *Nano Lett.* **2010**, *10*, 2609.
(23) Schmidt-Mende, L.; Zakeeruddin, S. M.; Gratzel, M. *Appl. Phys. Lett.* **2005**, 86.
(24) Bhongale, C. J.; Thelakkat, M. *Sol. Energy Mater. Sol. Cells* **2010**, *94*, 817.
(25) Vaynzof, Y.; Kabra, D.; Zhao, L.; Ho, P.; Wee, A.; Friend, R. *Appl. Phys. Lett.* **2010**, *97*, 033309.
(26) Savadogo, O.; Mandal, K. *Appl. Phys. Lett.* **1993**, *63*, 228.
(27) Lévy Clément, C.; Tena Zaera, R.; Ryan, M. A.; Katty, A.; Hodes, G. *Adv. Mater.* **2005**, *17*, 1512.
(28) Gregg, B.; Sprague, J.; Peterson, M. *J. Phys. Chem. B* **1997**, *101*, 5362.
(29) Peumans, P.; Yakimov, A.; Forrest, S. *J. Appl. Phys.* **2003**, *93*, 3693.
(30) Scully, S.; McGehee, M. *J. Appl. Phys.* **2009**, *100*, 034907.
(31) Jiang, X.; Österbacka, R.; Korovyanko, O.; An, C.; Horovitz, B.; Janssen, R.; Vardeny, Z. *Adv. Funct. Mater.* **2002**, *12*, 587.
(32) Hallermann, M.; Haneder, S.; Da Como, E. *Appl. Phys. Lett.* **2008**, 93.
(33) Kim, J. Y.; Kim, S. H.; Lee, H. H.; Lee, K.; Ma, W. L.; Gong, X.; Heeger, A. J. *Adv. Mater.* **2006**, *18*, 572.
(34) Street, R.; Schoendorf, M.; Roy, A.; Lee, J. *Phys. Rev. B* **2010**, *81*, 205307.
(35) Mihailetchi, V. D.; Wildeman, J.; Blom, P. W. M. *Phys. Rev. Lett.* **2005**, *94*, 126602.
(36) Yu, B. Y.; Tsai, A.; Tsai, S. P.; Wong, K. T.; Yang, Y.; Chu, C. W.; Shyue, J. J. *Nanotechnology* **2008**, *19*, 255202.
(37) Zeng, W.; Cao, Y.; Bai, Y.; Wang, Y.; Shi, Y.; Zhang, M.; Wang, F.; Pan, C.; Wang, P. *Chem. Mater.* **2010**, *22*, 1915.
(38) Weickert, J.; Sun, H.; Palumbiny, C.; Hesse, H. C.; Schmidt-Mende, L. *Sol. Energy Mater Sol. Cells* **2010**, *94*, 2371.
(39) Nezu, S.; Larramona, G.; Chone, C.; Jacob, A.; Delatouche, B.; Pere, D.; Moisan, C. *J. Phys. Chem. C* **2010**, *114* (14), 6854.